

See discussions, stats, and author profiles for this publication at: <https://www.researchgate.net/publication/282797212>

Complementary Semiconducting Polymer Blends (c-SPBs) for Efficient Charge Transport

ARTICLE *in* CHEMISTRY OF MATERIALS · OCTOBER 2015

Impact Factor: 8.35 · DOI: 10.1021/acs.chemmater.5b03349

READS

22

7 AUTHORS, INCLUDING:



Michael Roders

University of California, Santa Cruz

2 PUBLICATIONS 0 CITATIONS

[SEE PROFILE](#)



Jianguo Mei

Purdue University

40 PUBLICATIONS 2,750 CITATIONS

[SEE PROFILE](#)

Complementary Semiconducting Polymer Blends for Efficient Charge Transport

Yan Zhao,[†] Xikang Zhao,[†] Michael Roders,[‡] Ge Qu,[§] Ying Diao,[§] Alexander L. Ayzner,[‡] and Jianguo Mei^{*,†,||}

[†]Department of Chemistry, Purdue University, 560 Oval Drive, West Lafayette, Indiana 47907, United States

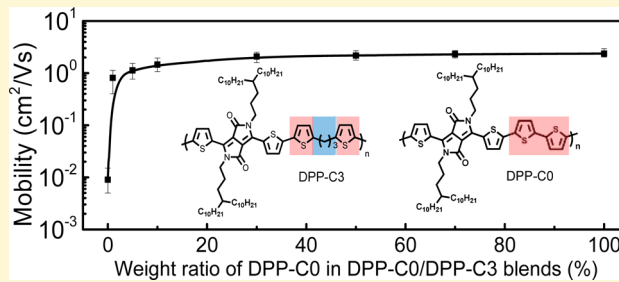
[‡]Department of Chemistry and Biochemistry, University of California at Santa Cruz, 1156 High Street, Santa Cruz, California 95064, United States

[§]Department of Chemical & Biomolecular Engineering, University of Illinois at Urbana-Champaign, 600 South Mathews Avenue, Urbana, Illinois 61801, United States

^{||}Birck Nanotechnology Center, Purdue University, 1205 West State Street, West Lafayette, Indiana 47906, United States

Supporting Information

ABSTRACT: Charge transport in polymeric thin films is a complicated process, which involves a multitude of coupled electronic events. Because of the growing appeal of semiconducting polymers in organic electronics, it makes the fundamental understanding of charge transport increasingly important. On the other hand, it urges the solution of the processability problem, frequently associated with high-performance polymers. In this study, we introduce complementary semiconducting polymer blends (*c*-SPBs), aiming to provide solutions for both the fundamental understanding of charge transport and the processability problem. The *c*-SPBs contain a highly crystalline matrix polymer with intentionally placed conjugation-break spacers (CBSs) along the polymer backbone, thus eliminating intrachain transport, and a tie chain polymer that is a fully conjugated polymer, restoring intrachain transport by connecting π -crystalline aggregates in the matrix polymer. The results show that the addition of as little as 1 wt % tie chain polymer into the matrix polymer induces a nearly 2 order of magnitude improvement in charge carrier mobility from ~ 0.015 to $1.14 \text{ cm}^2 \text{ V}^{-1} \text{ s}^{-1}$, accompanied by substantial lowering of activation energies from 100.1 to 64.6 meV. The morphological characterizations and electrical measurements confirm that tie chains are able to build the connectivity between crystalline aggregates, leading to efficient charge transport in the polymer blend films. Furthermore, this study suggests that *c*-SPBs can be a new platform for designing high-mobility electronic materials with enhanced solution processability for future organic electronics.



INTRODUCTION

Semiconducting polymers have been under extensive investigation because of their technological relevance in a wide range of applications from solar cells, light-emitting diodes, and transistors to various sensing platforms, among others.^{1–4} The capability of transporting charge carriers is one of the fundamental properties of semiconducting polymers. Efficient charge transport is strongly desired for such polymer-based thin-film devices, particularly for field-effect transistors (FETs) and organic circuits. To date, a great number of conjugated polymers have been reported with charge carrier mobilities of $> 1 \text{ cm}^2 \text{ V}^{-1} \text{ s}^{-1}$ in both p-type and n-type transistors.^{5–8} A handful of donor–acceptor-type (D–A) polymers have even shown hole mobility values exceeding $10 \text{ cm}^2 \text{ V}^{-1} \text{ s}^{-1}$.^{9–11} These inspiring and puzzling breakthroughs have far exceeded the charge transport limits for disordered polymers based on early theoretical models, mostly adapted from the study of inorganic semiconductors.^{12,13} The discrepancy between experimental results and theoretical predictions has triggered

a great deal of efforts in proposing new theories to explain the efficient charge transport behaviors in polymer thin films.¹⁴ For example, by studying an indacenodithiophene-benzothiadiazole copolymer, DeLongchamp et al. argued that charge transport in high-mobility semiconducting polymers is quasi one-dimensional (1D), predominantly occurring along the backbone. This requires only occasional intermolecular hopping through short π -stacking bridges.¹⁵ On the basis of studies with the same polymer, Sirringhaus et al. concluded that a planar, torsion-free polymer backbone with a low degree of energetic disorder is the origin for high charge carrier mobilities in donor–acceptor copolymers.¹⁶ Salleo et al. proposed a unified model of how charge carriers travel in conjugated polymer films from the study of a vast number of existing polymers. They argued that the limiting charge transport step is trapping caused by lattice

Received: August 27, 2015

Revised: October 4, 2015



disorder, and that short-range intermolecular aggregation is sufficient for efficient long-range charge transport. Hence, the unifying requirement for high carrier mobility is the presence of interconnected aggregates.¹² It was further proposed that there is an intrinsic molecular weight-dependent trade-off between paracrystallinity and connectivity in D-A polymer thin films. These studies and others provide new insights into charge transport in polymeric thin films and help in the design of the next generation. However, a comprehensive and coherent understanding of transport in polymeric thin films is still lacking, as there are questions that remain only partially addressed (e.g., charge percolation and electronic connectivity). More work is clearly needed to unlock the full potential of these materials for the next generation of flexible and printed electronic device applications.

In this study, we introduce complementary semiconducting polymer blends (*c*-SPBs), aiming to provide insights into charge transport from the aspect of materials design. The *c*-SPBs contain a highly crystalline matrix polymer with intentionally placed conjugation-break spacers along the polymer backbone, thus eliminating intrachain transport, and a tie chain polymer that is a fully conjugated polymer, restoring intrachain transport by connecting π -crystalline aggregates in the matrix polymer. We recognize that charge transport in polymer thin films is comprised of a complex series of events, which involve multiple electronic processes at different length scales. The contributions to charge transport arising from intrachain and interchain interactions contribute simultaneously to the charge mobility, and even approximately disentangling the individual contributions is challenging. For instance, the nature of the connections between π -aggregates is still poorly understood. We hypothesize that the disentanglement of intrachain and interchain interactions will be beneficial for the fundamental understanding of charge transport. It will also help to understand the proposed theoretical models, such as the tie chain model.¹⁷ Our approach involves the study of charge transport behaviors of a matrix polymer with intentionally placed conjugation-break spacers (CBSs) along the polymer backbones, thus eliminating intrachain transport. We then introduce various amounts of a fully conjugated polymer as the tie chain polymer into the polymer matrix, bringing back the efficient intrachain pathways. The results show that the addition of as little as 1 wt % tie chain polymer into the polymer matrix leads to a nearly 2 order of magnitude improvement in the charge carrier mobility from ~ 0.015 to $1.14 \text{ cm}^2 \text{ V}^{-1} \text{ s}^{-1}$, accompanied by a substantial lowering of the activation energy from 100.1 to 64.6 meV. The more tie chain polymer is added, the higher the mobility of the blend. We further performed a range of morphological characterizations and electrical measurements to validate the tie chain model in *c*-SPBs.

■ RESULTS AND DISCUSSION

DPP-C3 and DPP-C0 are the two model polymers under investigation, and their structures are shown in Figure 1. The synthesis and characterization of DPP-C3 and DPP-C0 have been previously reported.¹⁸ Briefly, DPP-C3 has a flexible, nonconjugated propyl spacer in the repeat unit, while DPP-C0 is a fully conjugated polymer. DPP-C3 formed highly crystalline two-dimensional (2D) lamellar aggregates in thin films with a step height of 2.2–2.4 nm. The highly crystalline nature of DPP-C3 thin films was also confirmed by grazing-incidence X-ray diffraction (GIXRD) measurements. The full width at half-maximum (fwhm) of both the lamellar and $\pi-\pi$ stacking peaks,

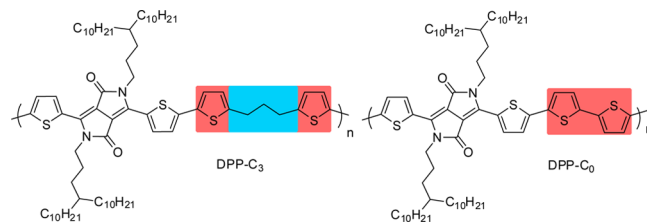


Figure 1. Chemical structures of DPP-C3 and DPP-C0.

i.e., the crystalline coherence length, in spin-coated films was reduced by approximately 25% in comparison with that of DPP-C0. The GIXRD measurement also revealed a lamellar spacing of 21.6 Å, in good agreement with the step height observed in the atomic force microscopy (AFM) experiment. In contrast, DPP-C0 has a rigid rod-like backbone. The strong $\pi-\pi$ interaction of conjugation planes drove the crystallization and helped form one-dimensional nanofibrillar aggregates with large aspect ratios, which is commonly observed in conjugated polymers. The HOMO levels for DPP-C0 and DPP-C3 are -4.97 and -5.13 eV, respectively, while LUMO energy levels are -3.65 and -3.73 eV, respectively.

Charge Transport Properties. The charge transport properties of DPP-C3 and DPP-C0 and their blends were evaluated by the bottom-gate bottom-contact field-effect transistors with silicon as the back gate electrode, a 300 nm thermally oxidized SiO_2 layer as the gate dielectric, and prepatterned gold electrodes as the source/drain (see Figure 2a). DPP-C3 ($M_n \sim 19.7$ kDa) showed an average hole mobility of $0.009 \text{ cm}^2 \text{ V}^{-1} \text{ s}^{-1}$ and a maximum at $0.015 \text{ cm}^2 \text{ V}^{-1} \text{ s}^{-1}$, extracted from the saturation regime in transistor transfer curves. These numbers are comparable to those obtained from widely investigated semicrystalline poly(3-hexylthiophene) (P3HT).^{19,20} Despite the absence of efficient intrachain charge transport pathways, DPP-C3 is still able to provide such an

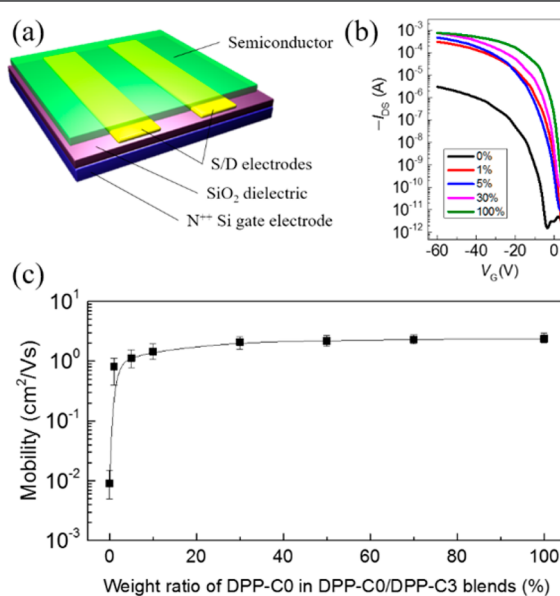


Figure 2. (a) Schematic bottom-gate bottom-contact devices on the Si/SiO_2 substrate used in this work. The channel length is $50 \mu\text{m}$, and the channel width is $1400 \mu\text{m}$. (b) Transfer curves for a representative device with a different polymer blend as the semiconductor layer. (c) Charge carrier mobility as a function of DPP-C0 weight ratio in the DPP-C0/DPP-C3 blends.

Table 1. Charge Transport Characteristics of DPP-C3 and the DPP-C0/DPP-C3 Blends in OFETs

DPP-C0:DPP-C3	μ_{max} ($\text{cm}^2 \text{ V}^{-1} \text{ s}^{-1}$)	μ_{avg} ($\text{cm}^2 \text{ V}^{-1} \text{ s}^{-1}$)	V_{th} (V)	$I_{\text{on}}/I_{\text{off}}$
0:100	0.015	0.009	-11.0 \pm 2.2	$\sim 10^6$
1:99	1.14	0.81	-9.6 \pm 1.8	10^7 – 10^8
5:95	1.54	1.13	-8.4 \pm 1.9	10^7 – 10^8
10:90	2.00	1.45	-7.9 \pm 0.6	$\sim 10^7$
30:70	2.52	2.09	-6.1 \pm 1.1	$\sim 10^7$
50:50	2.57	2.18	-4.9 \pm 1.9	$\sim 10^7$
70:30	2.90	2.30	-3.2 \pm 2.9	$\sim 10^7$
100:0	3.20	2.36	-2.0 \pm 2.4	10^6 – 10^7

intriguingly high mobility, suggesting that charge transport along π – π stacking directions is efficient in the π -stacks within a crystalline grain. On the other hand, long-range connectivity between the crystallites is missing in the DPP-C3 thin film because of a lack of conjugated tie chains. Connectivity between crystallites is essential for efficient charge transport, as demonstrated by various molecular weight experiments in the case of P3HT.¹⁷ To restore the connectivity, DPP-C0 ($M_n \sim 30.7$ kDa) was blended into DPP-C3 at ratios of 1, 5, 10, 30, 50, and 70 wt %. The field-effect transistor results are plotted in Figure 2 and summarized in Table 1 (see Figure S1 for electrical characteristics). Upon addition of 1 wt % DPP-C0, the mobility of the blend film nearly increased 2 orders of magnitude from 0.015 to $1.14 \text{ cm}^2 \text{ V}^{-1} \text{ s}^{-1}$, while it is only doubled from 1.54 to $3.20 \text{ cm}^2 \text{ V}^{-1} \text{ s}^{-1}$ with the DPP-C0 ratio increased from 5 to 100 wt %. To understand the underlying mechanism for these intriguing and puzzling findings, we have conducted the temperature-dependent FET mobility measurements.

Temperature-Dependent FET Characteristics. It is known that charge transport in conjugated polymers is generally an activated process, in which the activation energy—related to the polaron binding, self-trapping energy, or energetic disorder—is a fundamental quantity that is directly related to charge motion both along a single chain and between adjacent chains. To gain a better understanding of how the activation energy varies as a function of blend mole ratio, we performed temperature-dependent FET measurements in vacuum (below 1×10^{-3} Pa) in the temperature range of 125–300 K. The mobility–temperature curves from representative devices are shown in Figure 3a. Thermally activated charge transport behaviors were observed for all thin films.

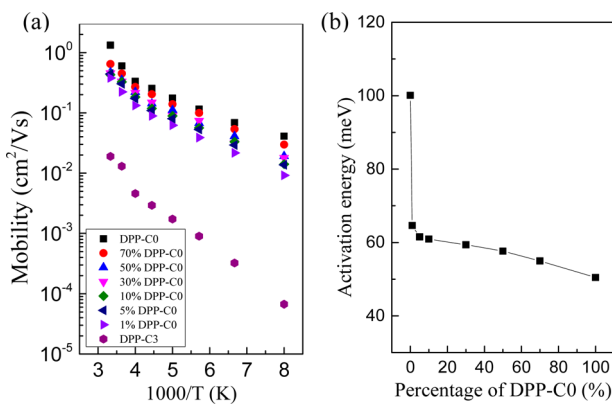


Figure 3. (a) Temperature-dependent field-effect mobilities for DPP-C3 and DPP-C0 and their blends. (b) Activation energy as a function of DPP-C0 ratio in DPP-C0/DPP-C3 blends.

That is, increased currents were obtained when the temperature was increased. At the same time, transistors still retained a high ON/OFF ratio and displayed saturation behavior. Activation energies were calculated from the temperature–mobility curves using the following relation:

$$\mu = \mu_0 e^{-E_A/kT}$$

where k is the Boltzmann constant, T is the thermodynamic temperature, E_A is the activation energy, μ is the T -dependent field-effect mobility, and μ_0 is the T -independent mobility prefactor, i.e., the mobility in the limit of high T . The calculated activation energies are plotted versus blend ratio in Figure 3b. The activation energy of the DPP-C3 thin film is around 100.1 meV. It quickly drops to 64.4 meV upon addition of 1 wt % DPP-C0. The activation energies continually drop from 61.5, 60.9, 59.4, 57.6, to 55.0 meV with an increase in the DPP-C0 ratio from 5, 10, 30, 50, to 70 wt % in the blend films (Table S1). The value extracted for the pure DPP-C0 thin film is 50.5 meV, in good agreement with reported values of DPP-based polymers.¹² The μ_0 values are also calculated by extrapolating $\log \mu$ versus $1/T$ lines to $1/T = 0$ (see Table S1). The μ_0 of DPP-C3 is much lower than that of DPP-C0, while the μ_0 values of the blend films increase slightly as the ratio of DPP-C0 increases. The trend observed in temperature-dependent FET measurements correlates well with charge transport properties of the blends, suggesting that the improvement in charge mobility is a result of lowering the activation energy in the polymer blends. To understand the cause of the lower activation energy in the blends, morphological investigations were performed.

Morphological Characterizations. As far as thin-film morphologies are concerned, two scenarios can occur in the blends. That is, DPP-C0 is distributed in the matrix of DPP-C3 (vice versa), or vertical phase segregation is present between DPP-C0 and DPP-C3 (e.g., DPP-C0 is lying underneath the DPP-C3 layer). Both scenarios could account for the improvement in charge transport and the drop in activation energy of the blends. Tapping mode AFM images of the blend films reveals that the addition of 1 wt % DPP-C0 did not lead to a noticeable change in the surface morphology of DPP-C3. The 1 wt % blend film still exhibits a 2D lamellar feature. Each layer is approximately ~ 2.2 – 2.4 nm thick, which is close to the lamellar spacing for DPP-C3 observed by GIXRD. With the blending ratio increasing from 5, 10, 30, 50, to 70 wt %, a gradual transition from 2D lamellar morphology to 1D fibril morphology is observed, as shown in Figure 4. The morphological findings suggest that vertical phase segregation is likely absent in the polymer blends. In contrast, vertical phase segregation is observed in the blends of DPP-C0 and polystyrene (see Figures S2 and S3), similar to the blends of P3HT and polystyrene (PS).^{21,22}

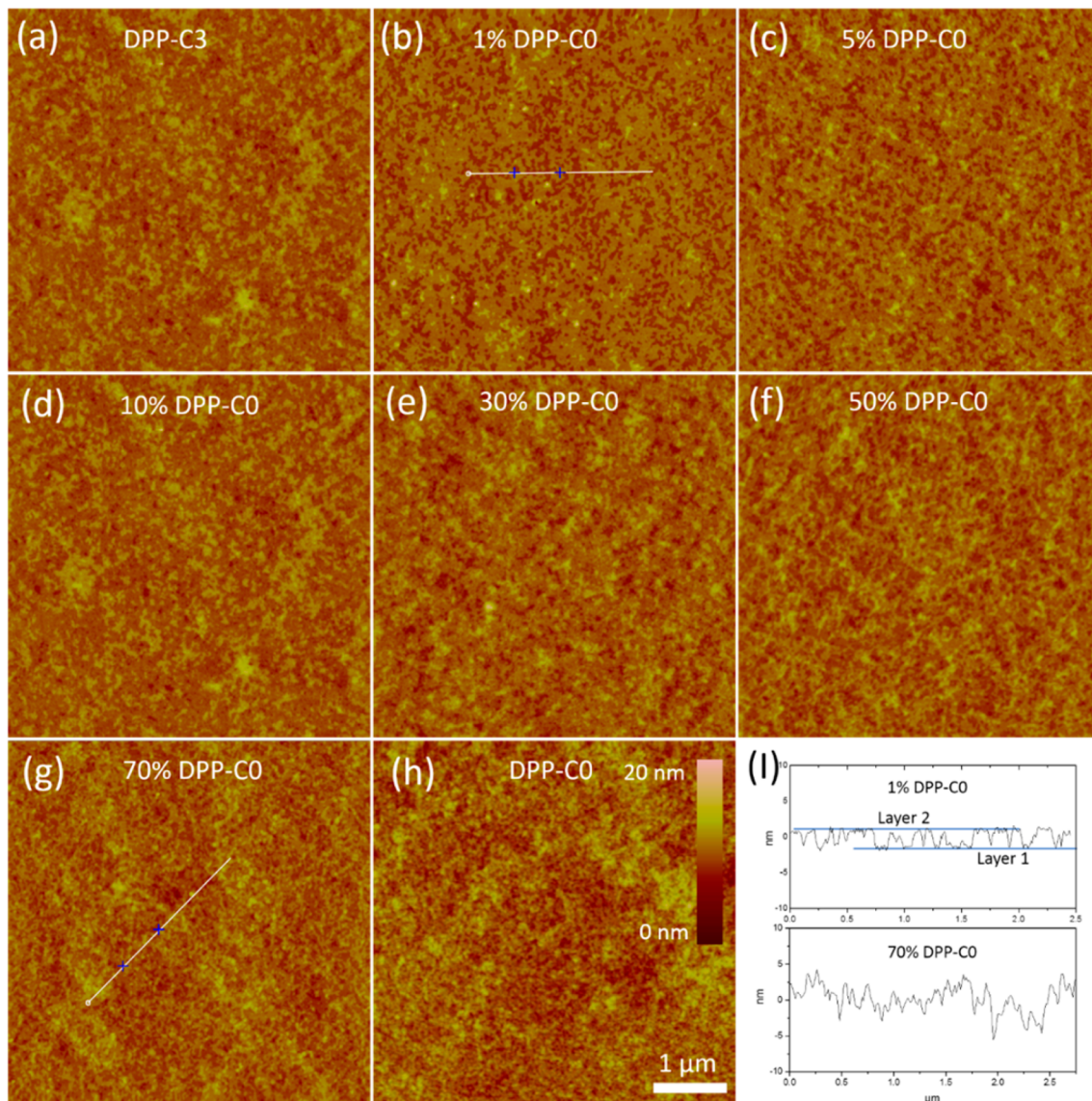


Figure 4. (a–h) AFM tapping mode images of polymer blend thin films. The polymer blend thin films were fabricated by spin coating on OTS-modified Si/SiO₂ substrates. The annealing temperature was 150 °C. (i) Cross-section images of panels b and g.

To explicitly rule out the possibility of vertical phase segregation in the blends of DPP-C0 and DPP-C3, sandwiched diode devices with an ITO/PEDOT (30 nm)/polymer film/MoO₃ (15 nm)/Ag (150 nm) configuration were fabricated. The assumption is that the space-charge limited current (SCLC) mobility would be largely limited by the layer of DPP-C3, if the vertical phase segregation is present in the polymer blends. We found out that SCLC mobility is actually proportional to the ratio of DPP-C0 in the blends, as shown in Figure S4. Briefly, The SCLC mobilities are 0.12×10^{-4} , 0.74×10^{-4} , 4.2×10^{-4} , and $26.9 \times 10^{-4} \text{ cm}^2 \text{ V}^{-1} \text{ s}^{-1}$ for the DPP-C0/DPP-C3 blends with DPP-C0 ratios of 0, 5, 50, and 100 wt %. The results strongly suggest vertical phase segregation is absent in the blends. Another piece of evidence comes from the measurement of the FET mobility of both sides of delaminated DPP-C0/DPP-C3 blend films, in which improvement in charge transport is found for both sides of the same film (see Figure S5).

Upon confirming that charge transport enhancement is not caused by vertical phase segregation, we next sought to answer

the question of whether the change in film morphology on mesoscopic length scales is the origin of enhanced charge mobilities. We performed grazing-incidence small-angle X-ray scattering (GISAXS) measurements on the blend polymer films. The 1D GISAXS intensity versus the scattering vector magnitude, Q , averaged over lateral film position, is plotted in Figure 5 on a double-logarithmic scale as a function of DPP-C0 mole fraction. We found that between 0 and 30% DPP-C0, the scattered intensity drops slightly but monotonically with DPP-C0 fraction, possibly because of subtle changes in the average electron density contrast in the blend film. To gain a rough sense of the characteristic size of the mean electron density inhomogeneities, we obtained the length scale d corresponding to the “knee” of the curve, where the slope changes near $Q \sim 0.03 \text{ Å}^{-1}$, using $d = 2\pi/Q$. As is clear from Figure 5, d is similar for all the curves between 0 and 30% ($22.5 \pm 0.7 \text{ nm}$ with no obvious trend). However, at larger mole fractions of DPP-C0, the intensity versus Q profile begins to change qualitatively. This is shown in the inset of Figure 5, which displays curves for 0, 50, and 100% DPP-C0. The 100% curve (pure DPP-C0 film,

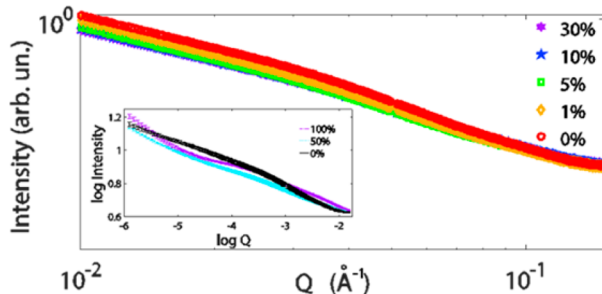


Figure 5. GISAXS results for polymer blend films. The different curves are for the weight percentages of DPP-C0 in the DPP-C0/DPP-C3 blends.

purple) approaches the “knee” region with a smaller slope, suggesting a more well-defined Guinier plateau region and thus a more defined characteristic particle size, which is still similar to that of DPP-C3. At low Q , the intensity drops more rapidly for DPP-C3, potentially because of another Guinier plateau corresponding to a larger aggregate size outside of the measured Q window. The curve for the 50% blend qualitatively lies somewhere between the 0 and 100% extremes, showing that the microstructure of DPP-C3 smoothly evolves from the pure polymer through the polymer blend and finally to that of pure DPP-C0. This rules out the possibility of a phase-segregated DPP-100/DPP-C0 network coexistence. Therefore, changes in mesoscale microstructure cannot alone account for the steep rise in charge mobilities at as little as 1% DPP-C0.

In addition, we performed grazing-incidence X-ray diffraction (GIXRD) measurements on DPP-C3 and the blend with a small fraction of DPP-C0 (1 wt %). It is found that the addition of DPP-C0 leads to a marginal change in the film morphology but lowers crystallinity from the DPP-C3 pure film to the 1 wt % blend film, as shown in Figure 6. Quantitative analysis of the

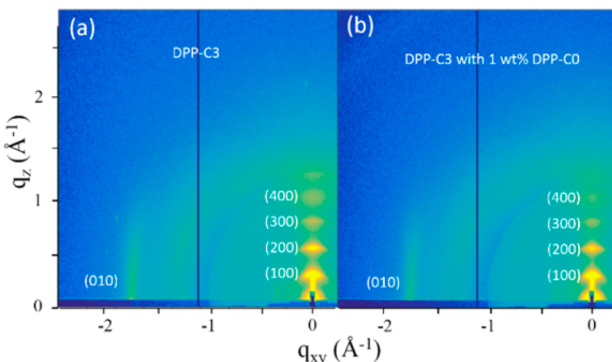


Figure 6. GIXRD images of (a) a pure DPP-C3 film and (b) a blend film of DPP-C3 with 1 wt % DPP-C0. The GIXRD images shown are prior to geometrical correction to allow direct comparison of the lamella peak intensities. The analysis is instead performed with proper geometrical correction.

$\pi-\pi$ stacking peak indicates that the relative degree of crystallinity decreased by approximately 30% with the addition of 1 wt % DPP-C0. The decrease in crystallinity is also evident from the reduced intensity of the higher-order lamella stacking peak, which is particularly apparent from (300) and (400) peaks. The totality of structural characterization allows us to conclude that the mobility enhancement at low mole fractions of DPP-C0 is not due to significant improvement in the nanoscale molecular packing of DPP-C3, or mesoscale phase

segregation (e.g., the formation of DPP-C0 nanowires) in the blends, as supported by GIXRD or GISAXS, respectively.

On the other hand, a relevant question may arise here. Can the DPP-C0 (1 wt %) itself form an interconnected network that is responsible for the efficient charge transport ($\sim 1 \text{ cm}^2 \text{ V}^{-1} \text{ s}^{-1}$) in the blend? In the absence of vertical phase segregation and without the participation of DPP-C3 crystalline aggregates, we expect this contribution would be insignificant for the lack of continuous charge transport pathways.²¹ To be more convincing, we prepared DPP-C20 with a conjugation-break spacer of 20 carbons, as shown in Figure 7. DPP-C20

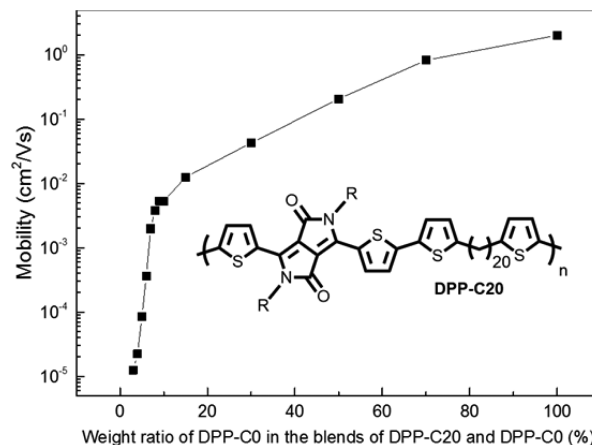


Figure 7. Charge carrier mobility as a function of DPP-C0 weight ratio in the DPP-C0/DPP-C20 blends.

itself does not exhibit any FET performance, because of the extended conjugation-break spacer. We then blended various ratios of DPP-C0 into DPP-C20. It is found that no FET performance was observed for the DPP-C0 (1 wt %)/DPP-C20 blend either. Not until 3 wt % DPP-C0 had been added into the DPP-C20 was a mobility of $10^{-5} \text{ cm}^2 \text{ V}^{-1} \text{ s}^{-1}$ obtained for the DPP-C0/DPP-C20 blend. This value is ~ 5 orders of magnitude lower than that of DPP-C0 (1 wt %) and DPP-C3. As much as 70 wt % DPP-C0 is needed in the blend to increase the mobility to the level of DPP-C0 (1 wt %) and DPP-C3. This control study clearly confirms that DPP-C0 (1 wt %) itself alone cannot form an effective interconnected network and is not responsible for the observed charge transport in the blend of DPP-C0 (1 wt %) and DPP-C3.

Understanding Charge Transport Enhancement in c-SPBs and Their Benefits. Combining morphological characterizations and electrical measurements, we conclude that (1) molecular π -stacks are formed in the crystalline π -aggregates in DPP-C3, which provides efficient charge transport pathways within a crystalline grain along the $\pi-\pi$ stacking direction, (2) charge transport between crystalline grains is limited in the DPP-C3 thin films because of the absence of intramolecular charge transport provided by extended π -conjugation, (3) tie chains (isolated DPP-C0 chains or small aggregates), even as low as 1 wt %, can build effective connectivity between crystalline aggregates, and (4) the efficient charge transport in the blends is a result of the interactions between tie chains and π -crystalline aggregates. The whole mechanistic process is illustrated in Figure 8. A similar mechanistic description has been proposed through the study of molecular weight effects using poly(3-hexylthiophene) (P3HT) on charge transport by McCulloch, Salleo, and

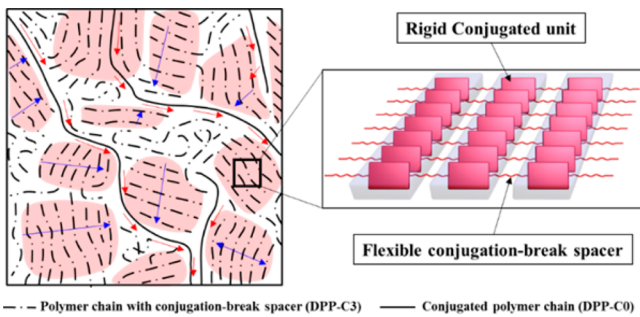


Figure 8. Schematic illustration of a complementary binary polymer blend thin film for efficient charge transport.

others.^{17,23,24} This study clearly proves the significance of connectivity with the invention of *c*-SPBs, a two-stage process by adding tie chains (DPP-C0) into the polymer matrix (DPP-C3). Furthermore, it is noted from the control experiment that the population of the crystalline π -stacks also plays a very important role in charge transport. In the case of DPP-C20 blends, a small percentage of DPP-C0 tie chain and dilute crystalline π -stacks in the DPP-C20 matrix are not able to form an effective interconnected network for efficient charge transport.

In addition to improving our mechanistic understanding of charge transport, most encouragingly, the use of a *c*-SPB offers an opportunity to lift intrinsic and general trade-offs in semicrystalline polymers. High-molecular weight polymers are typically desired for charge transport, because long chains build electrical connectivity between crystalline grains and allow efficient charge transport across crystalline boundaries. On the other hand, long chains are often associated with higher degrees of structural (paracrystalline) disorder in the π -stacking directions, leading to the formation of charge carrier traps.¹² Hence, charge transport is limited by paracrystalline disorder once connectivity between crystalline aggregates is sufficiently present. In this study, we have shown that a *c*-SPB could present both high crystallinity and necessary connectivity for efficient charge transport, where only a small percentage of conjugated tie chain polymer (DPP-C0) is blended into a highly crystalline polymer matrix (DPP-C3). We envision that such a *c*-SPB could ultimately provide superior charge transport characteristics to either of the individual components with the careful design of polymer pairs and optimization of the blend morphology.

Furthermore, a practical benefit for use of a *c*-SPB is to take advantage of the enhanced solution processability of the blends. As widely recognized, poor solution processability is a leading factor for batch-to-batch variation in synthesis and device fabrication. It imposes a serious threat to the commercialization of polymer-based organic electronics. Because of the presence of flexible conjugation-break spacers along its polymer backbone, DPP-C3 is highly soluble in common organic solvents. For instance, it has a solubility of >50 mg/mL in dichlorobenzene. In contrast, the solubility of DPP-C0 is ~3 mg/mL. In the blend system, only a small amount of fully conjugated polymer is required to build the connectivity. Therefore, solubility is no longer a problem during materials processing and device fabrication.

CONCLUSIONS

In summary, we have devised complementary semiconducting polymer blends to elucidate the role of connectivity in efficient charge transport in polymeric thin films. Our findings suggest that *c*-SPBs can be a new platform for investigating the fundamentals of charge transport, as well as for designing high-performance electronic materials with enhanced solution processability for future organic electronics. We are currently interested in probing where DPP-C0 chains reside in the matrix of DPP-C3, at boundaries of the π -aggregates or entering the aggregates, and how exactly charge carriers travel between tie chains and crystalline aggregates. In addition, we also plan to systematically investigate the impact of the π -stack population on charge transport through varying the conjugation-break spacer length.

ASSOCIATED CONTENT

S Supporting Information

The Supporting Information is available free of charge on the ACS Publications website at DOI: [10.1021/acs.chemmater.5b03349](https://doi.org/10.1021/acs.chemmater.5b03349).

Device fabrication, transistor characteristics, optical spectra, and contact-angle measurement ([PDF](#))

AUTHOR INFORMATION

Corresponding Author

*E-mail: jgmei@purdue.edu.

Notes

The authors declare no competing financial interest.

ACKNOWLEDGMENTS

The authors acknowledge the financial support from Purdue University. GISAXS measurements were taken at the Stanford Synchrotron Radiation Laboratory, a national user facility operated by Stanford University on behalf of the U.S. Department of Energy, Office of Basic Energy Sciences. GIXRD measurements were taken at the Advanced Photon Source, Argonne National Laboratory. We thank Professor Bryan Boudouris for sharing instruments in his laboratory for measuring the temperature-dependent transistor devices.

REFERENCES

- (1) Beaujuge, P. M.; Fréchet, J. M. J. Molecular Design and Ordering Effects in π -Functional Materials for Transistor and Solar Cell Applications. *J. Am. Chem. Soc.* **2011**, *133*, 20009–20029.
- (2) Mei, J.; Diao, Y.; Appleton, A. L.; Fang, L.; Bao, Z. Integrated Materials Design of Organic Semiconductors for Field-Effect Transistors. *J. Am. Chem. Soc.* **2013**, *135*, 6724–6746.
- (3) Grimsdale, A. C.; Leok Chan, K.; Martin, R. E.; Jokisz, P. G.; Holmes, A. B. Synthesis of Light-Emitting Conjugated Polymers for Applications in Electroluminescent Devices. *Chem. Rev.* **2009**, *109*, 897–1091.
- (4) Zhu, C.; Liu, L.; Yang, Q.; Lv, F.; Wang, S. Water-Soluble Conjugated Polymers for Imaging, Diagnosis, and Therapy. *Chem. Rev.* **2012**, *112*, 4687–4735.
- (5) Holliday, S.; Donaghey, J. E.; McCulloch, I. Advances in Charge Carrier Mobilities of Semiconducting Polymers Used in Organic Transistors. *Chem. Mater.* **2014**, *26*, 647–663.
- (6) Dong, H.; Fu, X.; Liu, J.; Wang, Z.; Hu, W. 25th Anniversary Article: Key Points for High-Mobility Organic Field-Effect Transistors. *Adv. Mater.* **2013**, *25*, 6158–6183.

- (7) Usta, H.; Facchetti, A.; Marks, T. J. n-Channel semiconductor materials design for organic complementary circuits. *Acc. Chem. Res.* **2011**, *44*, 501–10.
- (8) Zhao, Y.; Guo, Y.; Liu, Y. 25th Anniversary Article: Recent Advances in n-Type and Ambipolar Organic Field-Effect Transistors. *Adv. Mater.* **2013**, *25*, 5372–5391.
- (9) Kang, I.; Yun, H.-J.; Chung, D. S.; Kwon, S.-K.; Kim, Y.-H. Record High Hole Mobility in Polymer Semiconductors via Side-Chain Engineering. *J. Am. Chem. Soc.* **2013**, *135*, 14896–14899.
- (10) Tseng, H.-R.; Phan, H.; Luo, C.; Wang, M.; Perez, L. A.; Patel, S. N.; Ying, L.; Kramer, E. J.; Nguyen, T.-Q.; Bazan, G. C.; Heeger, A. J. High-Mobility Field-Effect Transistors Fabricated with Macroscopic Aligned Semiconducting Polymers. *Adv. Mater.* **2014**, *26*, 2993–2998.
- (11) Li, J.; Zhao, Y.; Tan, H. S.; Guo, Y.; Di, C.-A.; Yu, G.; Liu, Y.; Lin, M.; Lim, S. H.; Zhou, Y.; Su, H.; Ong, B. S. A stable solution-processed polymer semiconductor with record high-mobility for printed transistors. *Sci. Rep.* **2012**, *2*, 754.
- (12) Noriega, R.; Rivnay, J.; Vandewal, K.; Koch, F. P. V.; Stingelin, N.; Smith, P.; Toney, M. F.; Salleo, A. A general relationship between disorder, aggregation and charge transport in conjugated polymers. *Nat. Mater.* **2013**, *12*, 1038–1044.
- (13) Noriega, R.; Salleo, A. Charge Transport Theories in Organic Semiconductors. In *Organic Electronics II*; Wiley-VCH Verlag GmbH & Co. KGaA: Weinheim, Germany, 2012; pp 67–104.
- (14) Mollinger, S. A.; Krajina, B. A.; Noriega, R.; Salleo, A.; Spakowitz, A. J. Percolation, Tie-Molecules, and the Microstructural Determinants of Charge Transport in Semicrystalline Conjugated Polymers. *ACS Macro Lett.* **2015**, *4*, 708–712.
- (15) Zhang, X.; Bronstein, H.; Kronemeijer, A. J.; Smith, J.; Kim, Y.; Kline, R. J.; Richter, L. J.; Anthopoulos, T. D.; Sirringhaus, H.; Song, K.; Heeney, M.; Zhang, W.; McCulloch, I.; DeLongchamp, D. M. Molecular origin of high field-effect mobility in an indacenodithiophene–benzothiadiazole copolymer. *Nat. Commun.* **2013**, *4*, 2238.
- (16) Venkateshvaran, D.; Nikolka, M.; Sadhanala, A.; Lemaur, V.; Zelazny, M.; Kepa, M.; Hurhangee, M.; Kronemeijer, A. J.; Pecunia, V.; Nasrallah, I.; Romanov, I.; Broch, K.; McCulloch, I.; Emin, D.; Olivier, Y.; Cornil, J.; Beljonne, D.; Sirringhaus, H. Approaching disorder-free transport in high-mobility conjugated polymers. *Nature* **2014**, *515*, 384–388.
- (17) Himmelberger, S.; Vandewal, K.; Fei, Z.; Heeney, M.; Salleo, A. Role of Molecular Weight Distribution on Charge Transport in Semiconducting Polymers. *Macromolecules* **2014**, *47*, 7151–7157.
- (18) Zhao, Y.; Zhao, X.; Zang, Y.; Di, C.-a.; Diao, Y.; Mei, J. Conjugation-Break Spacers in Semiconducting Polymers: Impact on Polymer Processability and Charge Transport Properties. *Macromolecules* **2015**, *48*, 2048–2053.
- (19) Sirringhaus, H.; Tessler, N.; Friend, R. H. Integrated Optoelectronic Devices Based on Conjugated Polymers. *Science* **1998**, *280*, 1741–1744.
- (20) Bao, Z.; Dodabalapur, A.; Lovinger, A. J. Soluble and processable regioregular poly(3-hexylthiophene) for thin film field-effect transistor applications with high mobility. *Appl. Phys. Lett.* **1996**, *69*, 4108–4110.
- (21) Qiu, L.; Lim, J. A.; Wang, X.; Lee, W. H.; Hwang, M.; Cho, K. Versatile Use of Vertical-Phase-Separation-Induced Bilayer Structures in Organic Thin-Film Transistors. *Adv. Mater.* **2008**, *20*, 1141–1145.
- (22) Goffri, S.; Muller, C.; Stingelin-Stutzmann, N.; Breiby, D. W.; Radano, C. P.; Andreasen, J. W.; Thompson, R.; Janssen, R. A. J.; Nielsen, M. M.; Smith, P.; Sirringhaus, H. Multicomponent semiconducting polymer systems with low crystallization-induced percolation threshold. *Nat. Mater.* **2006**, *5*, 950–956.
- (23) Gasperini, A.; Sivula, K. Effects of Molecular Weight on Microstructure and Carrier Transport in a Semicrystalline Poly-(thieno)thiophene. *Macromolecules* **2013**, *46*, 9349–9358.
- (24) Chang, J.-F.; Clark, J.; Zhao, N.; Sirringhaus, H.; Breiby, D. W.; Andreasen, J. W.; Nielsen, M. M.; Giles, M.; Heeney, M.; McCulloch, I. Molecular-weight dependence of interchain polaron delocalization and exciton bandwidth in high-mobility conjugated polymers. *Phys. Rev. B: Condens. Matter Mater. Phys.* **2006**, *74*, 115318.